



# Discovery of New Fusion Inhibitor Peptides against SARS-CoV-2 by Targeting the Spike S2 Subunit

Mahmoud Kandeel<sup>1,2,\*</sup>, Mizuki Yamamoto<sup>3</sup>, Hideki Tani<sup>4</sup>, Ayako Kobayashi<sup>3</sup>, Jin Gohda<sup>3</sup>, Yasushi Kawaguchi<sup>3,5</sup>, Byoung Kwon Park<sup>6</sup>, Hyung-Joo Kwon<sup>6,\*</sup>, Jun-ichiro Inoue<sup>7,\*</sup> and Abdallah Alkattan<sup>1</sup>

<sup>1</sup>Department of Biomedical Sciences, College of Veterinary Medicine, King Faisal University, Al-Ahsa 31982, Saudi Arabia

<sup>2</sup>Department of Pharmacology, Faculty of Veterinary Medicine, Kafrelsheikh University, Kafrelsheikh 33516, Egypt

<sup>3</sup>Research Center for Asian Infectious Diseases, Institute of Medical Science, The University of Tokyo, Tokyo 108-8639, Japan

<sup>4</sup>Department of Virology, Toyama Institute of Health, Toyama 939-0363, Japan

<sup>5</sup>Division of Molecular Virology, Department of Microbiology and Immunology, The Institute of Medical Science, The University of Tokyo, Tokyo 108-8639, Japan

<sup>6</sup>Department of Microbiology, Hallym University College of Medicine, Chuncheon 24252, Republic of Korea

<sup>7</sup>Senior Professor Office, The University of Tokyo, Tokyo 108-8639, Japan

## Abstract

A novel coronavirus, severe acute respiratory syndrome coronavirus-2 (SARS-CoV-2), caused a worldwide pandemic. Our aim in this study is to produce new fusion inhibitors against SARS-CoV-2, which can be the basis for developing new antiviral drugs. The fusion core comprising the heptad repeat domains (HR1 and HR2) of SARS-CoV-2 spike (S) were used to design the peptides. A total of twelve peptides were generated, comprising a short or truncated 24-mer (peptide #1), a long 36-mer peptide (peptide #2), and ten peptide #2 analogs. In contrast to SARS-CoV, SARS-CoV-2 S-mediated cell-cell fusion cannot be inhibited with a minimal length, 24-mer peptide. Peptide #2 demonstrated potent inhibition of SARS-CoV-2 S-mediated cell-cell fusion at 1  $\mu$ M concentration. Three peptide #2 analogs showed IC<sub>50</sub> values in the low micromolar range (4.7-9.8  $\mu$ M). Peptide #2 inhibited the SARS-CoV-2 pseudovirus assay at IC<sub>50</sub>=1.49  $\mu$ M. Given their potent inhibition of viral activity and safety and lack of cytotoxicity, these peptides provide an attractive avenue for the development of new prophylactic and therapeutic agents against SARS-CoV-2.

**Key Words:** SARS-CoV-2, COVID-19, Fusion inhibitors, Antiviral drugs

## INTRODUCTION

The SARS-CoV-2 pandemic that began in 2019 has posed a significant threat worldwide. In the past two decades, three coronaviruses have emerged and endangered public health, including the severe acute respiratory syndrome coronavirus (SARS-CoV), Middle East respiratory syndrome CoV (MERS-CoV), and SARS-CoV-2 (Peeri *et al.*, 2020). Until the moment, there is no approved drug for treating SARS-CoV-2 infection. Therefore, discovery of new potential chemotherapeutics is an urgent demand.

The viral CoV genome encodes four structural proteins:

spike, membrane (M), envelope (E), and nucleocapsid (N). Viral membrane fusion is an essential step of virus replication, which is accomplished by the viral spike and leads to the fusion of the viral and cell membranes (Bosch *et al.*, 2003). The CoV S protein is composed of two subunits, S1 and S2. S1 binds the host cell angiotensin-converting enzyme-2 (ACE2) receptor (Song *et al.*, 2018; Hoffmann *et al.*, 2020). Cleavage of S1 by host cell proteases exposes a highly hydrophobic membrane-binding domain of the S2 subunit (Kirchdoerfer *et al.*, 2016). The S2 subunit contains two domains, heptad repeat domain 1 (HR1) and heptad repeat domain 2 (HR2). HR1 forms a homotrimer exposing three hydrophobic pockets on

**Open Access** <https://doi.org/10.4062/biomolther.2020.201>

This is an Open Access article distributed under the terms of the Creative Commons Attribution Non-Commercial License (<http://creativecommons.org/licenses/by-nc/4.0/>) which permits unrestricted non-commercial use, distribution, and reproduction in any medium, provided the original work is properly cited.

Received Nov 6, 2020 Revised Dec 8, 2020 Accepted Dec 10, 2020

Published Online Jan 11, 2021

### \*Corresponding Authors

E-mail: mkandeel@kfu.edu.sa (Kandeel M), hjoonkwon@hallym.ac.kr (Kwon HJ), jun-i@ims.u-tokyo.ac.jp (Inoue J)

Tel: +966-056-891-8734 (Kandeel M), +82-33-248-2635 (Kwon HJ), +81-3-6409-2476 (Inoue J)

Fax: +966-013-589-6617 (Kandeel M), +82-33-241-3640 (Kwon HJ), +81-3-6409-2477 (Inoue J)

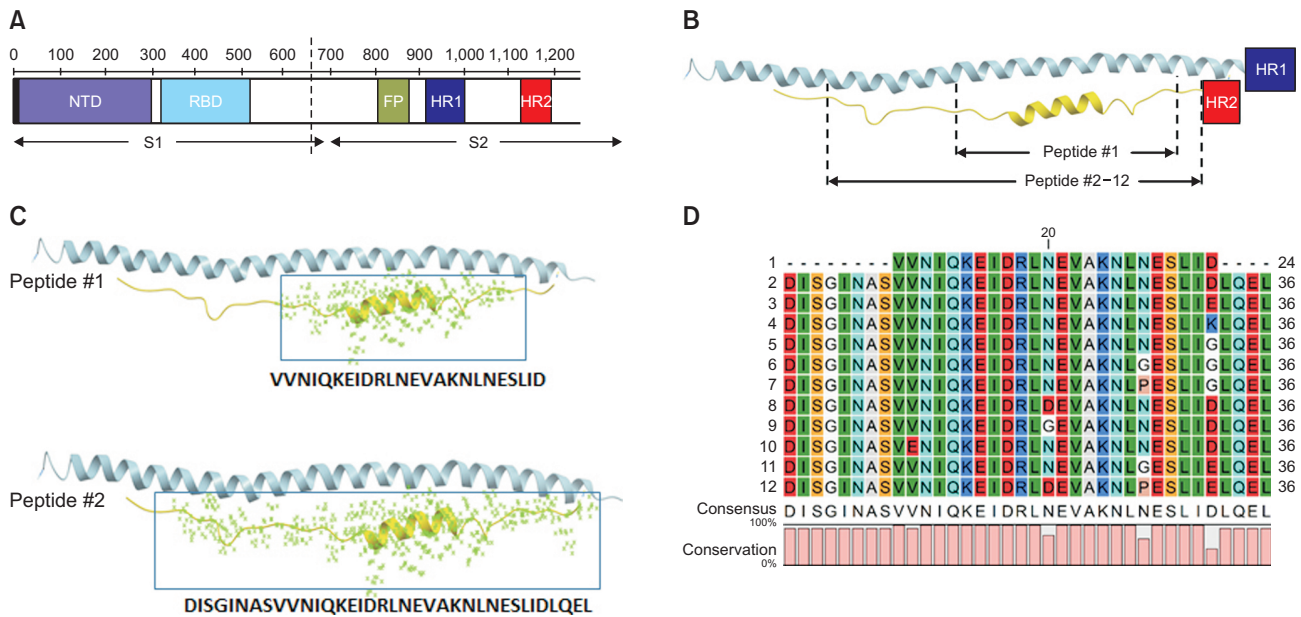


**Fig. 1.** The structure of SARS-CoV-2 fusion core and sequence of peptides. (A) Schematic representation of SARS-CoV-2 Spike. The S1 subunit contains the N-terminal domain (NTD) and the receptor-binding domain (RBD). The S2 subunit comprises the fusion protein (FP) and two heptad repeat domains, HR1 and HR2. (B) HR1 and HR2 monomers during the fusion state showing the regions comprising the synthesized. (C) The position of peptides #1 and 2 on HR2. The side chains of amino acids is presented in green dots. (D) The sequences of peptides #1-12, the conserved sequences were highlighted with the same colour.

its surface, which host the HR2 domain during the active fusion process (Xia *et al.*, 2014). An HR domain is composed of tandem repeat motifs of seven residues (named a-g). Of the seven residues, the first (a) and fourth (d) are predominantly hydrophobic or bulky (Gao *et al.*, 2013).

From a therapeutic perspective, fusion inhibitors have been successfully used in inhibiting viral infections as they harbor intrinsic ability to prevent the fusion of viral and cellular membranes. In this study, we investigated a current knowledge gap in the discovery of anti-SARS-CoV-2 fusion drugs. First, the inhibitory properties of a truncated 24-mer peptide (peptide #1) and a 36-mer peptide (peptide #2) were compared. The results indicated strong inhibition of S-mediated cell-cell fusion and SARS-CoV-2 pseudovirus activity. In addition, ten peptide #2 analogs were developed. The structural and molecular aspects of the associated inhibitory properties are discussed.

## MATERIALS AND METHODS

### Fusion peptides

Previous studies of SARS-CoV, MERS-CoV, and other viruses such as HIV and Ebola showed that HR1 analogs are usually weaker inhibitors than HR2-derived peptides (Liu *et al.*, 2004; Lu *et al.*, 2014; Shabane *et al.*, 2019). Furthermore, our previous work on developing MERS-CoV peptides showed that 36-amino acids HR2 analogs strongly inhibited MERS-CoV replication (Patent pending, USPTO application no. 16/857136). Previous studies on MERS-CoV peptides showed that a 19-mer peptide did not show any antiviral activity, and the 45-mer peptide demonstrated marginal activity (Lu *et al.*, 2014). Based on these data, we designed shorter 24-amino acid (peptide #1) and 36-amino acid (peptide #2)

HR2 analogs for potential anti-SARS-CoV2 activity. The concluded sequence for peptide synthesis was generated after alignment of SARS-CoV, SARS-CoV-2, and MERS-CoV HR2 sequences. The peptides were designed to include the central helix and residues on the extended N-terminal region (Fig. 1). In addition, a series of single or multiple modified peptide #2 analogs were produced by introducing a single, double, or triple amino acid mutation (Fig. 1). The mutations were based on the improvement of free energy of binding after amino acid mutations, as previously described (Dehouck *et al.*, 2013; Brender and Zhang, 2015). Each mutant residue was estimated to improve the binding energy by 0.1-0.5 kcal/mol. Peptide synthesis orders were sent to Apeptides (Shanghai, China) and Biomatik Inc (Ontario, Canada).

### Molecular dynamics simulations (MDs)

MDs were used to investigate the stability of the complex between the HR2-modified peptides #2-12 with HR1. The mutations were generated by Schrodinger Maestro package version 12 and saved as PDB files. MDs were performed as previously described with slight modifications (Kandeel *et al.*, 2018). GROMACS version 5.5.5 and GROMOS96 43a1 force field were used (Van Der Spoel *et al.*, 2005). The simulation continued for 10 ns to determine the root mean square deviation (RMSD) of the structure and the root mean square fluctuation (RMSF) of the residues. Snapshots were taken every 10 ps, providing 1000 snapshots for every complex.

### Cell lines and plasmids

HEK293T is an immortalized cell line derived from a human fetal kidney. A pair of previously described 293FT-based reporter cell lines that constitutively express individual split proteins (DSP1-7 and DSP8-11 proteins) (Wang *et al.*, 2014)

were used and maintained in Dulbecco's modified Eagle's medium (DMEM) containing 10% fetal bovine serum (FBS) and 1 g/mL puromycin. Calu-3 cells (ATCC HTB-55) were maintained in Eagle's minimum essential medium (EMEM) containing 10% fetal bovine serum (FBS). For the construction of transient transfection vectors, a synthetic DNA corresponding to the S gene of SARS-CoV-2 (NC\_045512.2) was cloned into a lentiviral transfer plasmid (CD500B-1, SBI, Palo Alto, CA, USA) and the VSV (Vesicular stomatitis virus)-G gene was cloned into pCAG plasmid.

### DSP assay to monitor membrane fusion

The DSP assay using 293FT cells was performed as described previously (Yamamoto *et al.*, 2020) to monitor SARS-CoV-2-S-mediated membrane fusion. Briefly, effector cells expressing SARS-CoV-2-S protein with DSP8-11, target cells expressing ACE2, and transmembrane serine protease 2 (TMPRSS2) with DSP1-7 were seeded in 10 cm culture dishes ( $4 \times 10^6$  cells/10 mL) one day before the assay. Two hours before the DSP assay, cells were treated with 6  $\mu$ M EnduRen (Promega, Madison, WI, USA), a substrate for Renilla luciferase, to activate EnduRen. One microliter of each peptide dissolved in dimethyl sulfoxide (DMSO) was added to the 384-well plates (Greiner Bioscience, Frickenhausen, Germany). Next, 50  $\mu$ L of each single-cell suspension (effector and target cells) was added to the wells using a Multidrop dispenser (Thermo Fisher Scientific, Waltham, MA, USA). After incubation at 37°C for 4 h, luciferase activity was measured using a Centro xS960 luminometer (Berthold, Bad-Wildbad, Germany).

### Preparation of pseudotyped VSV viral particles and infection experiments

293T cells were transfected with an expression plasmid for SARS-CoV-2-S, VSV-G, or control expression plasmid by calcium-phosphate precipitation. At 16 h posttransfection, the cells were inoculated with a replication-deficient VSV, VSV- $\Delta$ G-Luciferase, which lacks the VSV-G gene and encodes firefly luciferase, at an MOI=1 as described previously (Tani *et al.*, 2010). After 2 h of incubation, cells were washed with DMEM and further incubated for 16 h before supernatants containing the pseudotyped viral particles were harvested. Cellular debris was removed from the supernatants using a syringe filter with a 0.2  $\mu$ m size pore (Millipore, Bedford, MA, USA).

For an infection assay, target Calu-3 cells were seeded in 96-well plates ( $5 \times 10^4$  cells/100  $\mu$ L) one day before the assay. Cells were pre-treated with peptides for 1 h before infection. Pseudotyped viral particles were added to cells with the peptides. After 2 h of incubation, the culture supernatant was removed, and cells were washed with EMEM. Cells were further incubated in EMEM containing 10% FBS without peptides and pseudotyped viral particles. At 16 h postinfection, luciferase activity was measured using the Bright-Glo Luciferase Assay System (Promega) and Centro xS960 luminometer (Berthold).

### Statistical analysis

Statistically significant differences between the mean values were determined using a two-tailed Student's *t*-test. All data represent three independent experiments, and values represent the mean  $\pm$  standard deviation (SD), with  $p < 0.05$  considered statistically significant. Several correlation runs were conducted to evaluate the relationship between the ob-

tained activity and the molecular and structural descriptors of the peptides. Pearson's correlation coefficient and the degree of significance were estimated in GraphPad Prism software (GraphPad Software, San Diego, CA, USA).

## RESULTS

### The peptides sequences

The peptide design comprised testing the hypothesis of potential inhibition of SARS-CoV fusion by truncated or short peptide, a 24-mer (peptide #1). Furthermore, the 36-mer peptides were designed based on our previous research on MERS-CoV fusion as well as several fusion inhibition reports. All peptides contained the central helix of HR2 (Fig. 1). Peptides #2-12 contained several mutations of the WT 36-mer peptide #2 (Fig. 1). The inserted mutations were calculated to increase the binding free energy by  $\sim 0.5$  kcal/mol.

### DSP assay for SARS-CoV-2 S-mediated cell-cell fusion

We evaluated the effects of the twelve different peptides on SARS-CoV-2 S protein-mediated membrane fusion by DSP assay, which we previously established (Yamamoto *et al.*, 2020). Four peptides (#2, #3, #5 and #10) significantly reduced luciferase activity at 10  $\mu$ M in the DSP assay (Fig. 2A). Two peptides (#7 and #11) also reduced luciferase activity at 10  $\mu$ M with statistical meaning, although their inhibitory activities were much less than those of the four peptides listed above. The other six peptides did not affect luciferase activity. None of the twelve peptides affected luciferase activity in cells carrying the preformed DSP1-7/DSP8-11 reporter complex, indicating that luciferase activity under the treatment of each peptide in Fig. 2A reflects its effect on SARS-CoV-2 S mediated cell-cell fusion (Fig. 2B). Further analysis of the four peptides that strongly inhibited membrane fusion showed that Peptide #2 suppressed luciferase activity in a dose-response manner and exhibited the greatest inhibitory activity on the four peptides with a minimum IC<sub>50</sub> value at 1.0  $\mu$ M. (Fig. 2C, 2D). The IC<sub>50</sub> values of #3, #5, and #10 were 7.2, 4.7, and 8.9  $\mu$ M, respectively, indicating that the inhibitory activities of the three peptides were approximately 4- to 9-fold less than that of peptide #2 (Fig. 2D). Therefore, we chose peptide #2 for further analysis.

### The effect of peptide #2 on SARS-CoV-2-S pseudotyped VSV infection

We then examined the effect of peptide #2 on infection of human lung epithelial cells, Calu-3 cells with SARS-CoV-2-S, or VSV-G pseudotyped VSV viral particles. To analyze the effect of peptide #2 on the virus entry step, we treated Calu-3 cells with peptide #2 for 1 h before infection and for an additional 2 h during infection. After the pseudotyped viral particles were removed, cells were incubated for 16 h without the peptide to induce luciferase expression. The luciferase assay showed that the infectious activity of SARS-CoV-2-S pseudotyped viral particles was significantly suppressed by the treatment with peptide #2 (IC<sub>50</sub>=1.49  $\mu$ M) (Fig. 3A), while infection with VSV-G pseudotyped viral particles was not affected by peptide #2 (Fig. 3B). These results indicate that peptide #2 potently inhibits infection with SARS-CoV-2-S pseudotyped viral particles by preventing viral-cell fusion, possibly through binding of peptide #2 to the SARS-CoV-2 Spike.

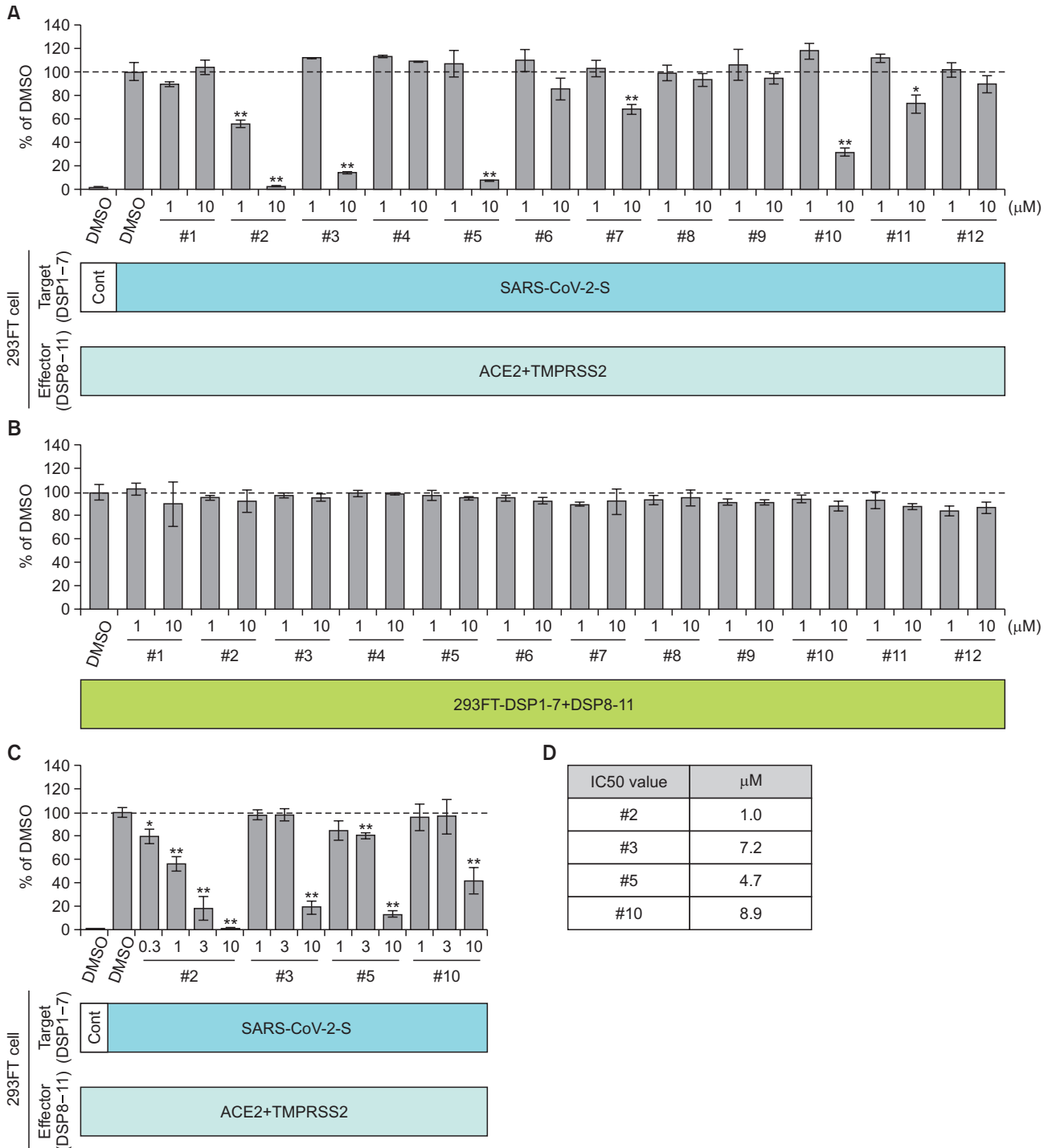


**Fig. 2.** The effect of peptides on SARS-CoV-2 S-mediated membrane fusion. (A) The effect of each peptides on the coculture fusion assay using DSP as a reporter. Peptides were tested at different concentrations, and the additional proteins other than reporters (DSPs) transduced into the effector and target cells are indicated below the graph. The relative cell fusion was represented as the DSP value (RL activity measured in RLU) normalized to that of the control assay with DMSO alone. (B) The effect of each peptides on RL measurement. Each peptides was added to cells co-expressing DSP1-7 and DSP8-11 to evaluate its direct inhibitory effects on RL. The relative DSP signal is indicated in the vertical axis by setting the control value with DSP alone as 100%. (C) Dose-response analysis for 5 peptides. The relative cell fusion was represented as the DSP value normalized to that of the control assay with DMSO alone. (D) Calculated IC50 value in figure (C). \* $p < 0.05$ , \*\* $p < 0.01$  vs. control assay with DMSO.

### Stability of peptides-HR1 complexes

The initial structure of the fusion complex contained a trimer of the 6-helix coiled-coil bundle of the HR1-HR2 fusion core. HR1 comprised the residues 912-989 of SARS-CoV S1, and HR2 contained 38 residues (1164-1202). MDs were used to evaluate the structural stability of the designed peptides and HR1 complexes. The RMSD of peptides-HR1 complexes is provided in Fig. 4A. Table 1 summarizes the average RMSD for every peptide-HR1 complex. The notable feature is the stability of the peptide complexes with low RMSD values (<0.2 nm). Overall, the results indicate tight binding of the peptides

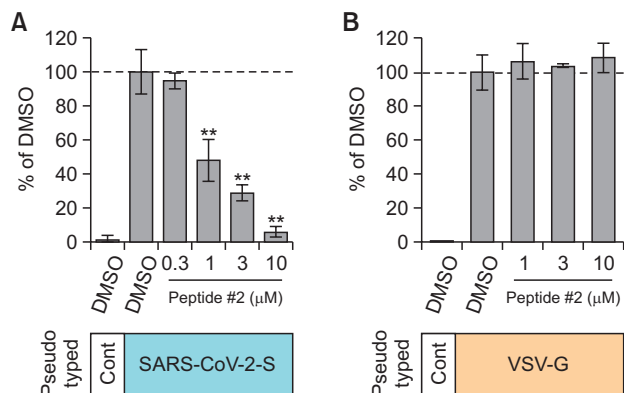


**Fig. 3.** The effect of peptide #2 on SARS-CoV-2 S-mediated viral infection. (A) The effect of peptide #2 on infection of Calu-3 cells with SARS-CoV-2 S pseudotyped VSV viral particles. The relative infectivity was represented as the RLU normalized to that of the control assay with DMSO alone. (B) The effect of peptide #2 on infection of Calu-3 cells with VSV-G pseudotyped VSV viral particles. The relative infectivity was represented as the RLU normalized to that of the control assay with DMSO alone. \*\* $p < 0.01$ .

complexes. RMSF values revealed that all peptides had a similar profile of low RMSF values, and the peak of high fluctuations corresponds to the loop connecting HR1 and HR2 (residues no. 70-80, Fig. 4B), as previously observed (Kandeel *et al.*, 2018).

The sequence and molecular descriptors of the composition of the peptides were analyzed to understand the observed inhibitory activity of the peptides on a molecular basis. In addition, multiple correlation analysis was adopted by investigating the relationship of each molecular descriptor with the corresponding activity (Table 2). Within the examined descriptors, only hydrophilic substitution showed a significant correlation with the obtained S-mediated cell-cell fusion % to DMSO ( $r = -0.63$ ,  $p < 0.05$ ) (Table 3).

### DISCUSSION

The discovery of new therapeutic agents against emerging viruses is the most effective tool to fight disease and decrease morbidity and mortality. In this context, fusion inhibitors have demonstrated substantial promise for both prophylaxis and treatment of viral infections. In this study, we introduced the first generation of small chemical molecules with anti-MERS-CoV fusion activity (Kandeel *et al.*, 2020b). Given the lack of approved anti-SARS-CoV-2 drugs, this study was conducted to initiate a drug discovery campaign by targeting the SARS-CoV-2 fusion step. Fusion inhibitors are commonly used for treating HIV. Currently, there are approximately 11 completed and one recruiting clinical trials for treating HIV patients with fusion inhibitors (<https://www.clinicaltrials.gov>). Fusion inhibition has been found a useful strategy to inhibit SARS-CoV (Liu *et al.*, 2004; Sainz *et al.*, 2006; Chu *et al.*, 2008; Liu *et al.*, 2009) and MERS-CoV (Lu *et al.*, 2014).

The virus entry inhibitors comprise two important steps of

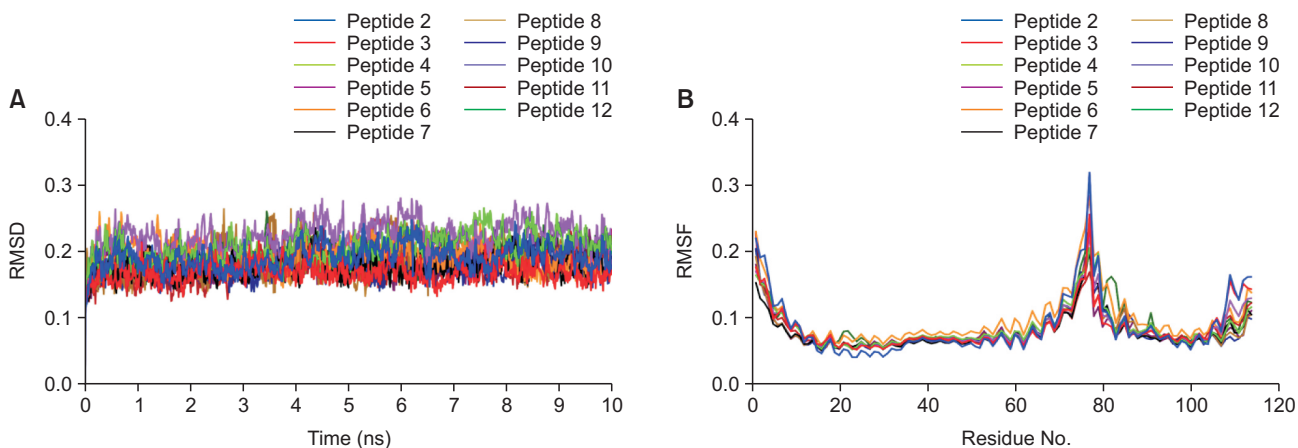


**Fig. 4.** Molecular dynamics simulation of the peptides #2-12 complexes with HR1. (A) RMSD plot showing the changes of the  $\alpha$ -carbon atom over the simulation time. (B) RMSF plot showing the fluctuations of the peptides-HR2 complex residues.

**Table 1.** The average RMSD values for peptides #2-12 after 10 ns molecular dynamics simulation

Peptide #	2	3	4	5	6	7	8	9	10	11	12
RMSD (nm)	0.192	0.169	0.208	0.189	0.195	0.179	0.194	0.176	0.181	0.176	0.193

**Table 2.** The protein structure statistics of the used peptides

ID	$\alpha$ -helix (residues)	$\alpha$ -helix %	Frequency of residues						Half-life in mammals (h)	%cell-cell fusion activity
			Negative charge	Positive charge	Other	Hydrophobic	Hydrophilic	Other		
# 2	7-34	75	0.194	0.083	0.722	0.444	0.28	0.28	1.1	3.078
# 3	7-34	75	0.194	0.083	0.722	0.444	0.28	0.28	1.1	13.694
# 4	7-34	75	0.167	0.111	0.722	0.444	0.28	0.28	1.1	108.542
# 5	7-34	75	0.167	0.083	0.75	0.472	0.278	0.25	1.1	7.609
# 6	7-34	75	0.167	0.083	0.75	0.5	0.25	0.25	1.1	85.133
# 7	7-25, 28-33	66.7	0.167	0.083	0.75	0.5	0.25	0.25	1.1	67.81
# 8	7-34	75	0.222	0.25	0.306	0.444	0.25	0.306	1.1	93.096
# 9	7-34	75	0.194	0.083	0.722	0.472	0.25	0.278	1.1	94.155
# 10	5-34	80.6	0.222	0.083	0.694	0.417	0.278	0.306	1.1	31.54
# 11	7-34	75	0.194	0.083	0.722	0.472	0.25	0.278	1.1	72.85
# 12	7-25, 27-34	69.4	0.222	0.083	0.694	0.472	0.222	0.306	1.1	89.708

**Table 3.** Correlation statistics of the obtained cell-cell fusion inhibition properties of the peptides with their sequence and molecular descriptors

	Activity% vs. $\alpha$ -helix %	Activity% vs. Negative charge	Activity% vs. Positive charge	Activity% vs. other charge	Activity% vs. hydrophobic	Activity% vs. hydrophilic	Activity% vs. other
Pearson r	-0.2782	0.02148	0.3442	-0.282	0.3148	-0.6326	0.1641
95% confidence interval	-0.7525 to 0.3861	-0.5859 to 0.6135	-0.3222 to 0.7825	-0.7543 to 0.3826	-0.3514 to 0.7694	-0.8934 to -0.05273	-0.4834 to 0.6955
R squared	0.07737	0.0004614	0.1184	0.07953	0.09911	0.4002	0.02692
<i>p</i> value							
<i>p</i> (two-tailed)	0.4075	0.9500	0.3000	0.4008	0.3457	0.0367	0.6298
<i>p</i> value summary	ns	ns	ns	ns	ns	*	ns
Significant? (alpha=0.05)	No	No	No	No	No	Yes	No
Number of XY pairs	11	11	11	11	11	11	11

the virus replication cycle: attachment and fusion. The viral receptor-binding domain (RBD) is an important attachment target for developing specific antiviral antibodies or vaccines. However, this target is prone to frequent mutation (Xia *et al.*, 2019). Therefore, fusion inhibitors target a highly conserved region in viral proteins.

Previous report revealed that CoVs can infect the cells via two entry mechanisms, direct membrane fusion or endocytosis (Qinfen *et al.*, 2004). SARS-CoV-2 entry can also be accomplished by both plasma membrane and endocytic pathways (Seyedpour *et al.*, 2020). Both mechanisms depend on the activation of the viral spike after cleavage, specifically, by a TMPRSS2 for plasma membrane pathway and the pH-dependent cysteine protease cathepsin L for the endocytic pathway. The pathways used for each cell line have been identified; for example, SARS-CoV-2 infects Calu-3 cells which endogenously express TMPRSS2 by the plasma membrane pathway and infects Vero cells which lacks expression of TMPRSS2 by the endocytic pathway (Hoffmann *et al.*, 2020). Since recent analysis of single-cell RNA-seq datasets from human tissues revealed that TMPRSS2 is expressed in a cell type specific manner (Sungnak *et al.*, 2020; Ziegler *et al.*, 2020). It is likely that the entry pathway also depends on the cell type. TMPRSS2-knockout resulted in reduced spread of SARS-

CoV and MERS-CoV in the airways accompanied by reduced severity of lung pathology in a mouse model (Iwata-Yoshikawa *et al.*, 2019). Therefore, TMPRSS2-dependent plasma membrane pathway is likely crucial for SARS-CoV-2 spread and disease development *in vivo*, and targeting plasma membrane pathway is likely to be an effective strategy to cure COVID-19. In this study, the S-mediated cell-cell fusion assay in TMPRSS2-expressing 293FT cells and pseudovirus assays in Calu-3 cells were dependent on TMPRSS2. Therefore, our results suggest that the peptides may inhibit the TMPRSS2-dependent plasma membrane pathway of the membrane fusion process.

In comparing the HR1-HR2 complexes, the SARS-CoV-2 complex has stronger binding energy than SARS-CoV, determined by the higher  $\alpha$ -helicity of HR1 (Zhu *et al.*, 2020). All peptides showed similar  $\alpha$ -helical content of 75% except #7 and #12, which demonstrated 66.7 and 69.4%, respectively (Table 1). A previous study determined that the enhanced  $\alpha$ -helical content of fusion peptides is associated with higher antiviral efficacy (Sainz *et al.*, 2006).

Both SARS and SARS-CoV-2 proteins demonstrate a high identity rate (Kandeel *et al.*, 2020a; Kandeel and Al-Nazawi, 2020). Experience from SARS-CoV fusion inhibitors shows that truncated peptides with a minimal length of 23-mer pep-

tides can inhibit the virus, which showed inhibition of fusion at IC<sub>50</sub> of 1.04 μM (Liu *et al.*, 2009). In this study, the truncated peptide #1 did not show significant inhibition. A 36-mer peptide of an HR analog strongly inhibited MERS-CoV S-mediated cell-cell fusion at 0.93 μM (Lu *et al.*, 2014). In this study, the 36-mer peptide #2 demonstrated potent inhibition of both SARS-CoV-2 S-mediated cell-cell fusion and pseudovirus activity at 1 and 1.4 μM, respectively. Novel antiviral compounds with IC<sub>50</sub> in the low micromolar range are expected to be promising lead structures (Liu *et al.*, 2004). Furthermore, the tested peptides were lacking any cytotoxicity suggesting their potential use in future drug discovery optimizations.

The use of peptide as chemotherapeutic agents has been widely applied in treating viral diseases e.g. HIV (Yao *et al.*, 2012), Zika virus (Jackman *et al.*, 2018), African swine fever virus (Hakobyan *et al.*, 2018), dengue virus (De La Guardia and Leonart, 2014), influenza virus (Kadam *et al.*, 2017) and feline immune deficiency virus (Mizukoshi *et al.*, 2009). Modifications of peptides had led to improvement of their systemic activity. For instance, amphipathic alpha helical peptides and cell penetrating peptides had improved the penetration of cell membranes and body barriers as blood brain barrier (Stalmans *et al.*, 2015). Engineering of peptides by using dextro-rotary (D)-amino acids improved the peptide stability and efficiency in delivery to remote organs (Garton *et al.*, 2018). The noninvasive methods of peptides delivery is now attracting the researchers' attention by oral, transdermal or nasal routes. Conjugation of peptides as insulin with polyarginines resulted in a dramatic increase in the systemic delivery after oral administration (Morishita *et al.*, 2007). Huge market potential for peptide-conjugates is expected, as well as there are several peptide drugs are now undergoing clinical trials (Vhora *et al.*, 2015). More recently, conjugation of peptides with polymeric, lipid and magnetic nanoparticles improved the systemic their delivery (Bashyal *et al.*, 2016). In the field of antiviral therapy, the antiviral fusion peptide enfuvirtide had been approved by FDA for treating HIV. This parent peptide has been used as a target for improved potency, stability, pharmacokinetics and drug delivery e.g. PEG conjugation (Cheng *et al.*, 2016), antithrombin-binding carrier pentasaccharide conjugates (Huet *et al.*, 2010) and transdermal delivery through low-frequency, low-Power ultrasound transducer patch (Snook *et al.*, 2019). Therefore, the promising advances in peptides therapy and delivery support the premise of using peptides in the treatment of SARS-CoV-2 infections.

In brief, this study investigated the discovery of new peptide inhibitors against SARS-CoV-2 fusion. Peptides # 2 inhibited S-mediated cell-cell fusion at 1 and 4.4 μM, respectively. This suggests the potent inhibition of SARS-CoV-2, probably by inhibition of the membrane fusion mechanism. Peptide #1 can be regarded as a lead compound for further antiviral optimization.

## CONFLICT OF INTEREST

The authors declare no conflict of interest.

## ACKNOWLEDGMENTS

The authors acknowledge the financial support from the

Administration of International Cooperation and Knowledge Exchange (ICKEA), King Faisal University, Project No. IC-01-20. This work was supported in part by grants-in-aid from the Japanese Society for the Promotion of Science (16H06575 to J. I., 20K07610 to M. Y.), a Program of Japan Initiative for Global Research Network on Infectious Diseases (JGRID) from AMED (JP20wm0125002 to Y. K.). The authors acknowledge the computational facilities at the college of veterinary medicine. King Faisal University.

## REFERENCES

- Bashyal, S., Noh, G., Keum, T., Choi, Y. W. and Lee, S. (2016) Cell penetrating peptides as an innovative approach for drug delivery; then, present and the future. *J. Pharm. Investig.* **46**, 205-220.
- Bosch, B. J., Van der Zee, R., De Haan, C. A. and Rottier, P. J. (2003) The coronavirus spike protein is a class I virus fusion protein: structural and functional characterization of the fusion core complex. *J. Virol.* **77**, 8801-8811.
- Breder, J. R. and Zhang, Y. (2015) Predicting the effect of mutations on protein-protein binding interactions through structure-based interface profiles. *PLoS Comput. Biol.* **11**, e1004494.
- Cheng, S., Wang, Y., Zhang, Z., Lv, X., Gao, G. F., Shao, Y., Ma, L. and Li, X. (2016) Enfuvirtide-PEG conjugate: a potent HIV fusion inhibitor with improved pharmacokinetic properties. *Eur. J. Med. Chem.* **121**, 232-237.
- Chu, L. H. M., Chan, S. H., Tsai, S. N., Wang, Y., Cheng, C. H. K., Wong, K. B., Waye, M. M. Y. and Ngai, S. M. (2008) Fusion core structure of the severe acute respiratory syndrome coronavirus (SARS-CoV): in search of potent SARS-CoV entry inhibitors. *J. Cell. Biochem.* **104**, 2335-2347.
- De La Guardia, C. and Leonart, R. (2014) Progress in the identification of dengue virus entry/fusion inhibitors. *BioMed Res. Int.* **2014**, 825039.
- Dehouck, Y., Kwasigroch, J. M., Rooman, M. and Gilis, D. (2013) BeAtMuSIC: prediction of changes in protein-protein binding affinity on mutations. *Nucleic Acid Res.* **41**, W333-W339.
- Gao, J., Lu, G., Qi, J., Li, Y., Wu, Y., Deng, Y., Geng, H., Li, H., Wang, Q. and Xiao, H. (2013) Structure of the fusion core and inhibition of fusion by a heptad repeat peptide derived from the S protein of Middle East respiratory syndrome coronavirus. *J. Virol.* **87**, 13134-13140.
- Garton, M., Nim, S., Stone, T. A., Wang, K. E., Deber, C. M. and Kim, P. M. (2018) Method to generate highly stable D-amino acid analogs of bioactive helical peptides using a mirror image of the entire PDB. *Proc. Natl. Acad. Sci. U.S.A.* **115**, 1505-1510.
- Hakobyan, A., Galindo, I., Nañez, A., Arabyan, E., Karalyan, Z., Chistov, A. A., Streshnev, P. P., Korshun, V. A., Alonso, C. and Zakaryan, H. (2018) Rigid amphipathic fusion inhibitors demonstrate antiviral activity against African swine fever virus. *J. Gen. Virol.* **99**, 148-156.
- Hoffmann, M., Kleine-Weber, H., Schroeder, S., Krüger, N., Herrler, T., Erichsen, S., Schiergens, T. S., Herrler, G., Wu, N. H., Nitsche, A., Müller, M. A., Drosten, C. and Pöhlmann, S. (2020) SARS-CoV-2 cell entry depends on ACE2 and TMPRSS2 and is blocked by a clinically proven protease inhibitor. *Cell* **181**, 271-280.e8.
- Huet, T., Kerbarh, O., Schols, D., Clayette, P., Gauchet, C., Dubreucq, G., Vincent, L., Bompais, H., Mazinghien, R., Querolle, O., Salvador, A., Lemoine, J., Lucidi, B., Balzarini, J. and Petitou, M. (2010) Long-lasting enfuvirtide carrier pentasaccharide conjugates with potent anti-human immunodeficiency virus type 1 activity. *Antimicrob. Agents Chemother.* **54**, 134-142.
- Iwata-Yoshikawa, N., Okamura, T., Shimizu, Y., Hasegawa, H., Takeda, M. and Nagata, N. (2019) TMPRSS2 contributes to virus spread and immunopathology in the airways of murine models after coronavirus infection. *J. Virol.* **93**, e01815-18.
- Jackman, J. A., Costa, V. V., Park, S., Real, A., Park, J. H., Cardozo, P. L., Ferhan, A. R., Olmo, I. G., Moreira, T. P., Bambirra, J. L., Queiroz, V. F., Queiroz-Junior, C. M., Foureaux, G., Souza, D.

- G., Ribeiro, F. M., Yoon, B. K., Wynendaele, E., De Spiegeleer, B., Teixeira, M. M. and Cho, N. J. (2018) Therapeutic treatment of Zika virus infection using a brain-penetrating antiviral peptide. *Nat. Mater.* **17**, 971-977.
- Kadam, R. U., Juraszek, J., Brandenburg, B., Buyck, C., Schepens, W. B., Kesteleyn, B., Stoops, B., Vreeken, R. J., Vermond, J. and Goutier, W. (2017) Potent peptidic fusion inhibitors of influenza virus. *Science* **358**, 496-502.
- Kandeel, M., Abdelrahman, A. H. M., Oh-Hashi, K., Ibrahim, A., Venugopala, K. N., Morsy, M. A. and Ibrahim, M. A. A. (2020a) Repurposing of FDA-approved antivirals, antibiotics, anthelmintics, antioxidants, and cell protectives against SARS-CoV-2 papain-like protease. *J. Biomol. Struct. Dyn.* doi: 10.1080/07391102.2020.1784291 [Online ahead of print].
- Kandeel, M. and Al-Nazawi, M. (2020) Virtual screening and repurposing of FDA approved drugs against COVID-19 main protease. *Life Sci.* **251**, 117627.
- Kandeel, M., Al-Taher, A., Li, H., Schwingschlogl, U. and Al-Nazawi, M. (2018) Molecular dynamics of Middle East Respiratory Syndrome Coronavirus (MERS CoV) fusion heptad repeat trimers. *Comput. Biol. Chem.* **75**, 205-212.
- Kandeel, M., Yamamoto, M., Al-Taher, A., Watanabe, A., Oh-Hashi, K., Park, B. K., Kwon, H. J., Inoue, J. I. and Al-Nazawi, M. (2020b) Small molecule inhibitors of Middle East respiratory syndrome coronavirus fusion by targeting cavities on heptad repeat trimers. *Biomol. Ther. (Seoul)* **28**, 311-319.
- Kirchdoerfer, R. N., Cottrell, C. A., Wang, N., Pallesen, J., Yassine, H. M., Turner, H. L., Corbett, K. S., Graham, B. S., McLellan, J. S. and Ward, A. B. (2016) Pre-fusion structure of a human coronavirus spike protein. *Nature* **531**, 118-121.
- Liu, I. J., Kao, C. L., Hsieh, S. C., Wey, M. T., Kan, L. S. and Wang, W. K. (2009) Identification of a minimal peptide derived from heptad repeat (HR) 2 of spike protein of SARS-CoV and combination of HR1-derived peptides as fusion inhibitors. *Antiviral Res.* **81**, 82-87.
- Liu, S., Xiao, G., Chen, Y., He, Y., Niu, J., Escalante, C. R., Xiong, H., Farmer, J., Debnath, A. K., Tien, P. and Jiang, S. (2004) Interaction between heptad repeat 1 and 2 regions in spike protein of SARS-associated coronavirus: implications for virus fusogenic mechanism and identification of fusion inhibitors. *Lancet* **363**, 938-947.
- Lu, L., Liu, Q., Zhu, Y., Chan, K. H., Qin, L., Li, Y., Wang, Q., Chan, J. F., Du, L., Yu, F., Ma, C., Ye, S., Yuen, K. Y., Zhang, R. and Jiang, S. (2014) Structure-based discovery of Middle East respiratory syndrome coronavirus fusion inhibitor. *Nat. Commun.* **5**, 3067.
- Mizukoshi, F., Baba, K., Goto, Y., Setoguchi, A., Fujino, Y., Ohno, K., Oishi, S., Kodera, Y., Fujii, N. and Tsujimoto, H. (2009) Antiviral activity of membrane fusion inhibitors that target gp40 of the feline immunodeficiency virus envelope protein. *Vet. Microbiol.* **136**, 155-159.
- Morishita, M., Kamei, N., Ehara, J., Isowa, K. and Takayama, K. (2007) A novel approach using functional peptides for efficient intestinal absorption of insulin. *J. Control. Release* **118**, 177-184.
- Peeri, N. C., Shrestha, N., Rahman, M. S., Zaki, R., Tan, Z., Bibi, S., Baghbanzadeh, M., Aghamohammadi, N., Zhang, W. and Haque, U. (2020) The SARS, MERS and novel coronavirus (COVID-19) epidemics, the newest and biggest global health threats: what lessons have we learned? *Int. J. Epidemiol.* **49**, 717-726.
- Qin, Z., Jinming, C., Xiaojun, H., Huanying, Z., Jicheng, H., Ling, F., Kunpeng, L. and Jingqiang, Z. (2004) The life cycle of SARS coronavirus in Vero E6 cells. *J. Med. Virol.* **73**, 332-337.
- Sainz, B., Jr., Mossel, E. C., Gallaher, W. R., Wimley, W. C., Peters, C. J., Wilson, R. B. and Garry, R. F. (2006) Inhibition of severe acute respiratory syndrome-associated coronavirus (SARS-CoV) infectivity by peptides analogous to the viral spike protein. *Virus Res.* **120**, 146-155.
- Seyedpour, S., Khodaei, B., Loghman, A. H., Seyedpour, N., Kisomi, M. F., Balibegloo, M., Nezamabadi, S. S., Gholami, B., Saghazadeh, A. and Rezaei, N. (2020) Targeted therapy strategies against SARS-CoV-2 cell entry mechanisms: a systematic review of *in vitro* and *in vivo* studies. *J. Cell. Physiol.* doi: 10.1002/jcp.30032 [Online ahead of print].
- Shabane, P. S., Izadi, S. and Onufriev, A. V. (2019) General purpose water model can improve atomistic simulations of intrinsically disordered proteins. *J. Chem. Theory Comput.* **15**, 2620-2634.
- Snook, K. A., Van Ess, R., 2nd, Werner, J. R., Clement, R. S., Ocon-Grove, O. M., Dodds, J. W., Ryan, K. J., Acosta, E. P., Zurlo, J. J. and Mulvihill, M. L. (2019) Transdermal delivery of enfuvirtide in a porcine model using a low-frequency, low-power ultrasound transducer patch. *Ultrasound Med. Biol.* **45**, 513-525.
- Song, W., Gui, M., Wang, X. and Xiang, Y. (2018) Cryo-EM structure of the SARS coronavirus spike glycoprotein in complex with its host cell receptor ACE2. *PLoS Pathog.* **14**, e1007236.
- Stalmans, S., Bracke, N., Wynendaele, E., Gevaert, B., Peremans, K., Burvenich, C., Polis, I. and De Spiegeleer, B. (2015) Cell-penetrating peptides selectively cross the blood-brain barrier *in vivo*. *PLoS ONE* **10**, e0139652.
- Sungnak, W., Huang, N., Bécavin, C., Berg, M., Queen, R., Litvinukova, M., Talavera-López, C., Maatz, H., Reichart, D., Sampaziotis, F., Worlock, K. B., Yoshida, M. and Barnes, J. L. (2020) SARS-CoV-2 entry factors are highly expressed in nasal epithelial cells together with innate immune genes. *Nat. Med.* **26**, 681-687.
- Tani, H., Shiokawa, M., Kaname, Y., Kambara, H., Mori, Y., Abe, T., Moriishi, K. and Matsuura, Y. (2010) Involvement of ceramide in the propagation of Japanese encephalitis virus. *J. Virol.* **84**, 2798-2807.
- Van Der Spoel, D., Lindahl, E., Hess, B., Groenhof, G., Mark, A. E. and Berendsen, H. J. (2005) GROMACS: fast, flexible, and free. *J. Comput. Chem.* **26**, 1701-1718.
- Vhora, I., Patil, S., Bhatt, P. and Misra, A. (2015) Chapter one - protein- and peptide-drug conjugates: an emerging drug delivery technology. In *Advances in Protein Chemistry and Structural Biology* (R. Donev, Ed.), Vol. 98, pp. 1-55. Academic Press.
- Wang, H., Li, X., Nakane, S., Liu, S., Ishikawa, H., Iwamoto, A. and Matsuda, Z. (2014) Co-expression of foreign proteins tethered to HIV-1 envelope glycoprotein on the cell surface by introducing an intervening second membrane-spanning domain. *PLoS ONE* **9**, e96790.
- Xia, S., Liu, Q., Wang, Q., Sun, Z., Su, S., Du, L., Ying, T., Lu, L. and Jiang, S. (2014) Middle East respiratory syndrome coronavirus (MERS-CoV) entry inhibitors targeting spike protein. *Virus Res.* **194**, 200-210.
- Xia, S., Yan, L., Xu, W., Agrawal, A. S., Algaissi, A., Tseng, C. K., Wang, Q., Du, L., Tan, W., Wilson, I. A., Jiang, S., Yang, B. and Lu, L. (2019) A pan-coronavirus fusion inhibitor targeting the HR1 domain of human coronavirus spike. *Sci. Adv.* **5**, eaav4580.
- Yamamoto, M., Kiso, M., Sakai-Tagawa, Y., Iwatsuki-Horimoto, K., Imai, M., Takeda, M., Kinoshita, N., Ohmagari, N., Gohda, J., Semba, K., Matsuda, Z., Kawaguchi, Y., Kawaoaka, Y. and Inoue, J. I. (2020) The anticoagulant nafamostat potentially inhibits SARS-CoV-2 S protein-mediated fusion in a cell fusion assay system and viral infection *in vitro* in a cell-type-dependent manner. *Viruses* **12**, 629.
- Yao, X., Chong, H., Zhang, C., Waltersperger, S., Wang, M., Cui, S. and He, Y. (2012) Broad antiviral activity and crystal structure of HIV-1 fusion inhibitor sifuvirtide. *J. Biol. Chem.* **287**, 6788-6796.
- Zhu, Y., Yu, D., Yan, H., Chong, H. and He, Y. (2020) Design of potent membrane fusion inhibitors against SARS-CoV-2, an emerging coronavirus with high fusogenic activity. *J. Virol.* **94**, e00635-20.
- Ziegler, C. G. K., Allon, S. J., Nyquist, S. K., Mbano, I. M., Miao, V. N., Tzouanas, C. N., Cao, Y., Yousif, A. S., Bals, J., Hauser, B. M., Feldman, J., Muus, C., Wadsworth, M. H., 2nd, Kazer, S. W., Hughes, T. K., Doran, B., Gatter, G. J., Vukovic, M., Taliaferro, F., Mead, B. E., Guo, Z., Wang, J. P., Gras, D., Plaisant, M., Ansari, M., Angelidis, I., Adler, H., Sucre, J. M. S., Taylor, C. J., Lin, B., Waghray, A., Mitsialis, V., Dwyer, D. F., Buchheit, K. M., Boyce, J. A., Barrett, N. A., Laidlaw, T. M., Carroll, S. L., Colonna, L., Tkachev, V., Peterson, C. W., Yu, A., Zheng, H. B., Gideon, H. P., Winchell, C. G., Lin, P. L., Bingle, C. D., Snapper, S. B., Kropski, J. A., Theis, F. J., Schiller, H. B., Zaragosi, L. E., Barby, P., Leslie, A., Kiem, H. P., Flynn, J. L., Fortuna, S. M., Berger, B., Finberg, R. W., Kean, L. S., Garber, M., Schmidt, A. G., Lingwood, D., Shalek, A. K. and Ordovas-Montanes, J. (2020) SARS-CoV-2 receptor ACE2 is an interferon-stimulated gene in human airway epithelial cells and is detected in specific cell subsets across tissues. *Cell* **181**, 1016-1035.e19.